Intronic locus determines *SHROOM3* expression and potentiates renal allograft fibrosis

Madhav C. Menon,[1] Peter Y. Chuang,[1] Zhengzhe Li,[1] Chengguo Wei,[1] Weijia Zhang,[1] Yi Luan,[1] Zhengzi Yi,[1] Huabao Xiong,[2] Christopher Woytovich,[1] Ilana Greene,[1] Jessica Overbey,[1] Ivy Rosales,[3] Emilia Bagiella,[1] Rong Chen,[4] Meng Ma,[4] Li Li,[4] Wei Ding,[4] Arjang Djamali,[5] Millagros Saminego,[6] Philip J. O'Connell,[7] Lorenzo Gallon,[8] Robert Colvin,[3] Bernd Schroppel,[1] John Cijiang He,[1,9] and Barbara Murphy[1]

[1]Division of Nephrology and [2]Clinical Immunology, Department of Medicine, Icahn School of Medicine at Mount Sinai, New York, New York, USA. [3]Department of Pathology, Massachusetts General Hospital, Harvard Medical School, Boston, Massachusetts, USA. [4]Department of Genetics and Genomic Sciences, Icahn School of Medicine at Mount Sinai, New York, New York, USA. [5]Nephrology, University of Wisconsin, Madison, Wisconsin, USA. [6]Nephrology, University of Michigan, Ann Arbor, Michigan, USA. [7]Renal Unit, University of Sydney at Westmead Hospital, Sydney, Australia. [8]Medicine-Nephrology and Surgery-Organ Transplantation, Northwestern University Feinberg School of Medicine, Chicago, Illinois, USA. [9]Renal Section, James J Peter Veterans Affairs Medical Center, New York, New York, USA.

Fibrosis underlies the loss of renal function in patients with chronic kidney disease (CKD) and in kidney transplant recipients with chronic allograft nephropathy (CAN). Here, we studied the effect of an intronic SNP in *SHROOM3*, which has previously been linked to CKD, on the development of CAN in a prospective cohort of renal allograft recipients. The presence of the rs17319721 allele at the *SHROOM3* locus in the donor correlated with increased *SHROOM3* expression in the allograft. In vitro, we determined that the sequence containing the risk allele at rs17319721 is a transcription factor 7–like 2–dependent (TCF7L2-dependent) enhancer element that functions to increase *SHROOM3* transcription. In renal tubular cells, TGF-β1 administration upregulated *SHROOM3* expression in a β-catenin/TCF7L2–mediated manner, while SHROOM3 in turn facilitated canonical TGF-β1 signaling and increased α1 collagen (*COL1A1*) expression. Inducible and tubular cell–specific knockdown of *Shroom3* markedly abrogated interstitial fibrosis in mice with unilateral ureteric obstruction. Moreover, *SHROOM3* expression in allografts at 3 months after transplant and the presence of the *SHROOM3* risk allele in the donor correlated with increased allograft fibrosis and with reduced estimated glomerular filtration rate at 12 months after transplant. Our findings suggest that rs17319721 functions as a *cis*-acting expression quantitative trait locus of *SHROOM3* that facilitates TGF-β1 signaling and contributes to allograft injury.

Introduction

Chronic kidney disease (CKD) affects 10% of adults in the US, and its incidence and prevalence are increasing worldwide (1). In addition to conferring risk for end-stage renal disease (ESRD), CKD increases the risk of cardiovascular disease and all-cause mortality (2). Tubulointerstitial fibrosis (TIF) is a final common pathogenic process for CKD from varied etiologies and is a primary component of chronic allograft nephropathy (CAN). CAN manifests as a progressive decline of renal function in the renal allograft (3, 4) and is the most common cause of death-censored long-term graft loss (5, 6). A significant percentage of patients with CKD or CAN will eventually progress to ESRD requiring dialysis or kidney transplantation (7). To date, there is no effective therapy to prevent the progression of CKD or CAN. Therefore, it is critical to identify new therapeutic targets for averting the development and progression of TIF.

GWAS in large CKD cohorts of predominantly European ancestry have strongly linked an intronic SNP in *SHROOM3*, rs17319721, to prevalent and incident CKD (8–10). *SHROOM3* encodes a PDZ domain–containing protein that binds F-actin and regulates its subcellular distribution (11, 12). However, the role of the SHROOM3 risk genotype in allograft injury and the role of SHROOM3 in kidney fibrosis and CKD are unknown.

In our ongoing, prospective, NIH-sponsored Genomics of Chronic Allograft Rejection study (GoCAR; ClinicalTrials.gov ID NCT00611702) in kidney transplant recipients, we performed protocol allograft biopsies at predetermined time points after transplantation and correlated renal allograft gene expression 3 months after transplantation to indices of allograft dysfunction at 12 months. Based on an initial observation, that the CKD-associated rs17319721 polymorphism in SHROOM3 altered *SHROOM3* expression, we performed a series of experiments to address mechanisms linking SHROOM3 to renal fibrosis and CAN. Our results indicated that the risk allele for *SHROOM3* confers higher SHROOM3 expression by facilitating Wnt/β-catenin–dependent, TCF7L2-mediated gene transcription. SHROOM3 augmented canonical TGF-β1/SMAD3 signaling, resulting in enhanced profibrotic gene expression. The clinical importance of the findings was determined by an observed significant relationship between allograft *SHROOM3* expression at 3 months (referred to herein as SHROOM3-3M), or the presence of the risk allele of rs17319721, and a higher risk of CAN in renal allograft recipients from the GoCAR cohort. In addition to providing a mechanism underly-

Conflict of interest: Arjang Djamali has received endowments from Bristol-Myers-Squibb, Takada-Millenium, and Sanofi.
Submitted: May 21, 2014; **Accepted:** October 31, 2014.
Reference information: *J Clin Invest*. 2015;125(1):208–221. doi:10.1172/JCI76902.

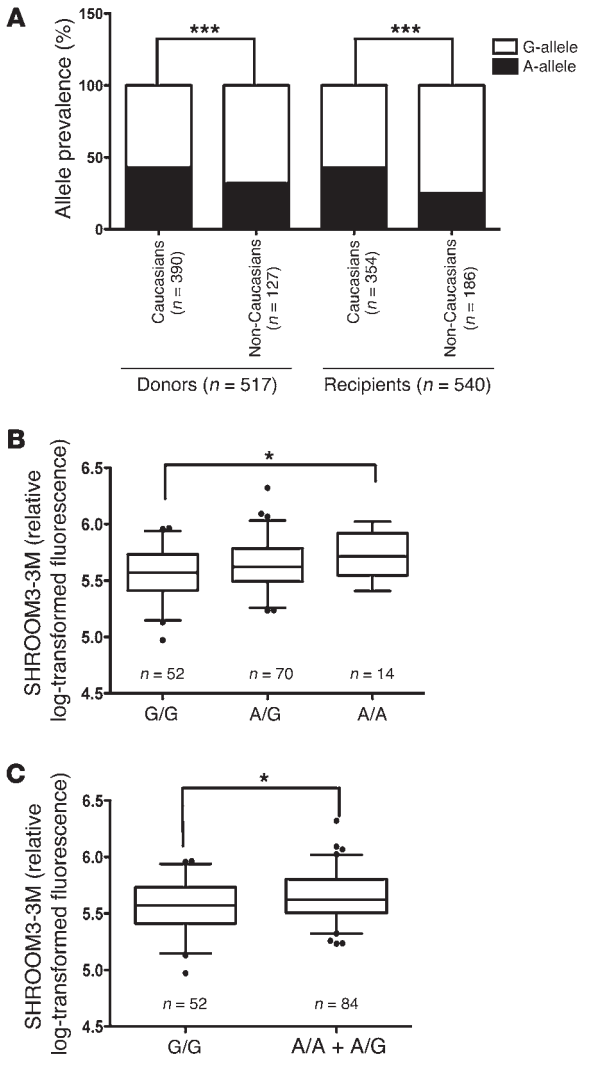

Figure 1. The A allele of rs17319721 in the donor is associated with higher allograft *SHROOM3* expression at 3 months and confers significantly higher CAN risk at 12 months. (**A**) Allele distribution at rs17319721 in Caucasian and non-Caucasian allograft donors and recipients in the GoCAR cohort, expressed as a percentage. ***$P < 0.0001$, χ^2 test. (**B**) Allograft SHROOM3-3M, grouped according to donor genotype. *$P < 0.05$ among groups, ANOVA; $P < 0.05$, A/A vs. G/G, unpaired *t* test. (**C**) SHROOM3-3M in allografts with 1 or 2 copies of the risk allele (A/A or A/G) compared with those without the risk allele (G/G). The presence of the A allele in the donor was associated with significantly greater CADI-12≥2 risk in all allografts (OR, 1.98; CI, 1.10–3.59) and in live donor allografts of Caucasian origin (OR, 5.41; CI, 1.56–18.39) (see Supplemental Table 1). *$P = 0.02$, unpaired *t* test. (**B** and **C**) SHROOM3-3M values are presented as log-transformed fluorescence relative to normal preperfusion biopsies. Line represents median; boxes represent interquartile range; whiskers represent 5th to 95th percentile; individual dots represent outliers.

ing the association between intronic rs17319721 SHROOM3 SNPs and progressive CKD and CAN, our results identified SHROOM3 as a potentially important therapeutic target to prevent kidney fibrosis and CAN.

Results

The A allele of rs17319721 in the donor is associated with higher allograft SHROOM3-3M. Multiple studies have now linked the rs17319721 *SHROOM3* SNP to CKD (8–10). Whether the risk allele is associated with altered *SHROOM3* expression in the renal parenchyma, or is related to CAN, is not known. As of January 1, 2013, 589 recipients were enrolled in the parent study, GoCAR. We performed targeted genotyping for this locus on 540 allograft recipients and 517 donors within the GoCAR cohort (Supplemental Figure 1A; supplemental material available online with this article; doi:10.1172/JCI76902DS1). Allelic prevalence of the CKD-associated A allele was 36.66% among recipients and 39.94% among donors. Overall, the prevalence of the A allele was similar for Caucasian donors and recipients (42.87% and 42.56%, respectively). The number of subjects in each non-Caucasian ethnicity (i.e., African-Americans, Asians, Hispanics, and others) was not sufficient to make valid inference about rs17319721 distribution.

In both recipients and donors, we observed that the prevalence of the A allele was significantly higher in Caucasians versus non-Caucasians ($P < 0.0001$; Figure 1A).

Next, we examined whether allograft SHROOM3-3M correlates with the presence of the A allele. Allograft gene expression microarray analysis from 3-month protocol biopsies was performed on 159 of the entire 589 enrollees in the GoCAR study. These patients represented by chronology the first 159 enrollees in GoCAR who were biopsied 3 months after transplantation (Table 1 and Supplemental Figure 1A). Targeted genotyping results for rs17319721 as well as *SHROOM3* transcript levels from kidney allografts were available from 136 donors and 145 recipients (Supplemental Figure 1A). We observed that SHROOM3-3M was significantly higher in allografts that were homozygous for the CKD risk allele (A/A, $n = 14$) compared with allografts that were homozygous for the G allele (G/G, $n = 52$; $P = 0.01$; Figure 1B). SHROOM3-3M was also significantly higher in allografts from donors with at least 1 risk allele (A/A or A/G, $n = 84$) compared with donors without the risk allele (G/G, $n = 52$; $P = 0.02$; Figure 1C). Interestingly, when we examined the relationship between SHROOM3-3M and the recipient's genotype, rather than the donor's, there was no significant correlation between the A allele and SHROOM3-3M ($n = 145$; Supplemental Figure 1B). To further confirm that the A allele in the donor was associated with increased SHROOM3-3M, we performed RT-PCR on 3-month biopsies (32 in the microarray and 21 in nonmicroarray; Supplemental Figure 1A) of patients for which we had available RNA. In these 53 patients, *SHROOM3* expression was significantly higher with the A allele (A/A or A/G) than without (G/G; Supplemental Figure 1C). When Caucasian donor allografts were separately examined, *SHROOM3* expression was higher with the A allele genotype by both microarray and RT-PCR ($P = 0.05$ and $P = 0.02$, respectively; Supplemental Figure 1, D and E). We next examined the relationship of the A allele to SHROOM3 expression in preperfusion baseline biopsies (SHROOM3-0M). In randomly selected RNA samples distributed among each genotype, we again identified higher SHROOM3 expression with the presence of the A allele, as well as a higher SHROOM3-0M with the A/A versus G/G genotype, by RT-PCR ($n = 10$ [A/A], 9 [A/G], 11 [G/G]; Supplemental Figure 1, F and G). These results confirmed the association of the A allele in the donor with increased allograft SHROOM3 expression.

Table 1. Baseline characteristics of the GoCAR and microarray cohorts

Parameter	GoCAR (*N* = 589)	Microarray (*N* = 159)	*P*
Recipient demographics			
Age (yr)[A]	50.17 ± 13.7 (18–83)	48.84 ± 13.27 (19–73)	0.27
Female	185 (31.41%)	47 (29.35%)	0.55
Caucasian	375 (63.67%)	92 (57.5%)	0.41
African-American	123 (20.88%)	37 (23.1%)	
Other race	91 (15.45%)	30 (19.1%)	
Donor demographics			
Age (yr)[A]	42.01 ± 15.2 (0–76)	41.13 ± 16.80 (3–76)	0.53
Female	278 (47.20%)	77 (48.13%)	0.86
Caucasian	451 (76.57%)	121 (75.6%)	0.77
African-American	57 (9.68%)	17 (10.63%)	
Other race	81 (13.75%)	21 (13.77%)	
Deceased	329 (55.86%)	95 (59.38%)	0.78
Living	260 (44.14%)	64 (41.62%)	
12-month biopsy measurements[B]			
CADI-12 (score)[A]		2.09 ± 2.49 (0–10)	
eGFR-12 (ml/min/1.73 m^2)[A]		58.12 ± 19.45 (10.6–109.2)	

Unless otherwise indicated, values represent *n* (%). [A]Mean ± SD (range). [B]CADI-12 was available for 101 subjects, and eGFR-12 for 147 subjects, from the microarray cohort at the time of publication.

Allograft SHROOM3-3M and the A allele of rs17319721 are associated with higher risk of CAN in renal allograft recipients. Since we observed that the A allele of rs17319721, previously associated with CKD, was also associated with increased *SHROOM3* transcription, we next examined whether SHROOM3-3M and/or the donor risk genotype correlated with indices of allograft dysfunction (CAN) at 12 months.

Allograft gene expression microarray analysis from 3-month protocol biopsies was performed on 159 of the entire 589 enrollees in the GoCAR study. At the time of publication, estimated glomerular filtration rate at 12 months (eGFR-12) was available in 147 subjects from the subgroup, and chronic allograft dysfunction index score at 12 months (CADI-12) was available in 101 subjects (Table 1 and Supplemental Figure 1A). Reasons for not having a 12-month biopsy in this subgroup included graft loss ($n = 8$), death ($n = 1$), loss to follow-up ($n = 9$), and contraindication for or inability to obtain a renal allograft biopsy ($n = 40$).

SHROOM3-3M correlated inversely with eGFR-12 ($r = -0.2192$, $P < 0.01$; Figure 2A) and positively with CADI-12 ($r = 0.2458$, $P = 0.03$; Figure 2B). This correlation remained significant ($P = 0.01$) after exclusion of 2 biopsies with diagnosis (BK virus nephropathy and severe cortical scarring). The relationship of SHROOM3-3M to CADI-12 and eGFR-12 was further validated by RT-PCR in the internal cohort of 32 subjects (eGFR-12, $r = -0.39$, $P = 0.02$; CADI-12, $r = 0.38$, $P = 0.03$; Supplemental Figure 2, A and B). A robust correlation existed between *SHROOM3* expressions from microarray and quantitative RT-PCR ($P = 0.0008$; Supplemental Figure 2C). No correlation existed, however, between SHROOM3-3M and simultaneous CADI-3 ($n = 135$; Supplemental Figure 2D). In multivariate analysis, SHROOM3-3M was predictive of CADI-12 of at least 2 (CADI-12≥2) and inversely related to eGFR-12 (Supplemental Tables 1 and 2). Among covariates included in the analysis, acute rejection before 3 months had significant independent effects on CADI-12 and eGFR-12 ($P < 0.05$).

To corroborate that SHROOM3-3M is associated with progression of CAN, we compared SHROOM3-3M between allografts that had ≥2 increase in CADI score between 3- and 12-month biopsies (ΔCADI≥2, termed progressors; $n = 17$), and those with <2 increase in CADI score (ΔCADI<2, termed nonprogressors; $n = 68$). SHROOM3-3M was significantly higher in progressors versus nonprogressors ($P = 0.04$; Figure 2C). Furthermore, allografts in the highest quartile of SHROOM3-3M sustained a significantly greater fall in eGFR between 3- and 12-month biopsies compared with those in the lowest quartile (Supplemental Figure 2E).

Next, we examined the donor risk genotype and its association with CAN. At the time of analysis for the present study, 203 subjects of the GoCAR cohort had available CADI-12: 101 from the microarray cohort and 102 from the nonmicroarray cohort (Supplemental Figure 1A). In this group, the presence of the A allele in the donor was associated with a significantly greater risk of CADI-12≥2 in all allografts (odds ratio [OR], 1.98; CI, 1.10–3.59; Supplemental Table 3), indicating a higher risk of CAN with the risk allele.

Correlation of SHROOM3 expression with CAN progression is affected by race. Since the *SHROOM3* SNP has been linked with CKD in predominantly Caucasian cohorts (8, 9), we sought to determine whether the relationship observed between SHROOM3-3M, or the A allele, and CAN also follows a racial predilection. In the microarray cohort, 109 Caucasian donor allografts had available eGFR-12 and 80 had available CADI-12. SHROOM3-3M correlated inversely with eGFR-12 ($r = -0.2712$, $P < 0.01$; Figure 2D) and directly with CADI-12 ($r = 0.255$, $P = 0.02$; Figure 2E). In multivariate analysis of Caucasian donor allografts, SHROOM3-3M was still significantly predictive of CADI-12≥2 and low eGFR-12 outcomes (Supplemental Tables 1 and 2). In non-Caucasian allografts, SHROOM3-3M was not significantly correlated with either eGFR-12 ($n = 38$) or CADI-12 ($n = 21$) (Supplemental Figure 2, F and G). Of the 85 allograft recipients that had both CADI-3 and CADI-12 available, 70 received Caucasian donor allografts, and we compared the SHROOM3-3M among progressors and nonprogressors of these recipients. SHROOM3-3M for the 14 progressors was significantly higher than the 56 nonprogressors (Figure 2F). Among allografts in the GoCAR cohort with both donor genotype and CADI-12, the presence of the A allele in the donor was associated with increased CAN risk (i.e., CADI-12≥2) among allografts of Caucasian origin from live donors (OR, 5.41; CI, 1.56–18.39; Supplemental Table 3). Since the etiology of CAN is multifactorial, we generated logistic models, including clinical predictors, to predict the outcomes of CADI-12≥2 and ΔCADI≥2. To minimize the effect of baseline disease on subsequent histological progression, we excluded allografts with CADI-3 greater than 3 from the model for CADI progressors. For these outcomes, we generated 2 categories of models — clinical and demographic predictors in each model either with or without SHROOM3-3M in different subgroups. We identified that the AUC for prediction of high CADI-12 and ΔCADI were improved in each subgroup when SHROOM3-3M was added, more so in Caucasian donors (Supplemental Table 4).

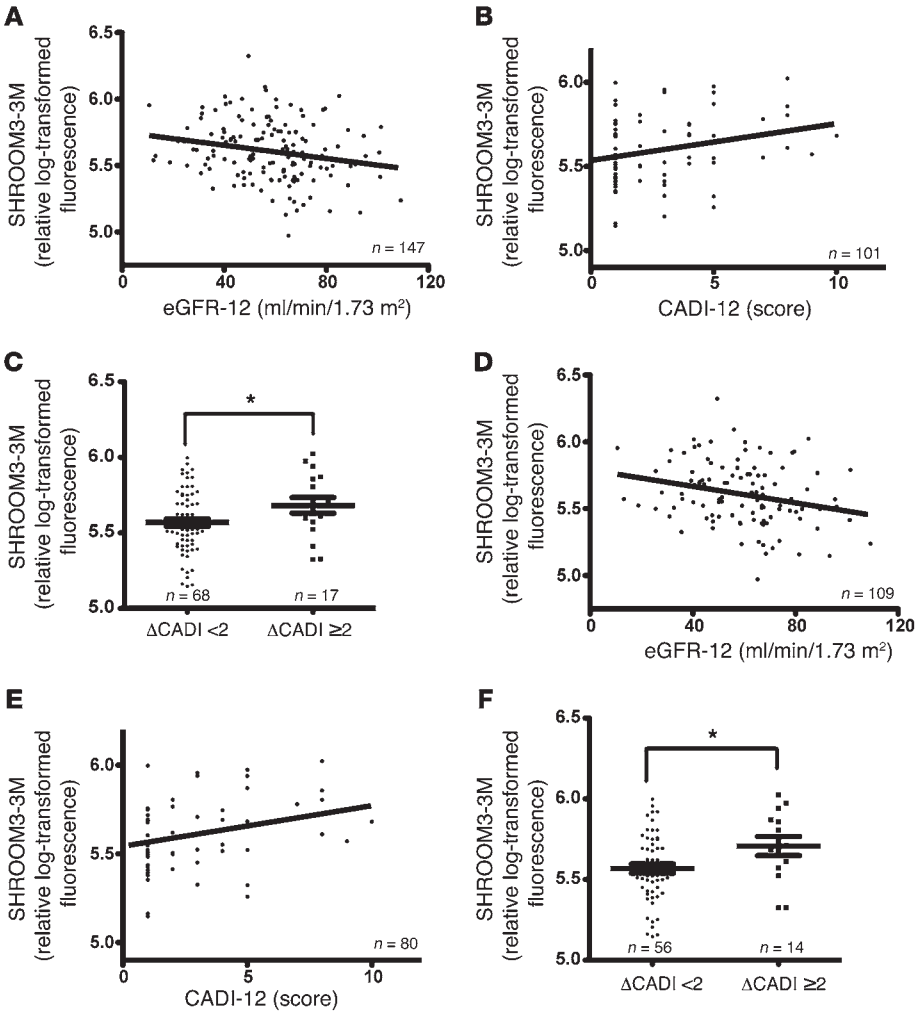

Figure 2. Upregulation of *SHROOM3* antedates and correlates with indices of allograft dysfunction in Caucasian donor allografts. (**A** and **B**) Correlation of allograft SHROOM3-3M with eGFR-12 ($r = -0.20$, $P = 0.01$) (**A**) and with allograft CADI-12 ($r = 0.22$, $P = 0.02$) (**B**). (**C**) SHROOM3-3M in nonprogressors (ΔCADI<2) and progressors (ΔCADI≥2). (**D** and **E**) Correlation of SHROOM3-3M to eGFR-12 ($r = -0.25$; $P < 0.01$; **D**) and to CADI-12 ($r = 0.25$; $P = 0.02$; **E**) in recipients of Caucasian donor kidneys. (**F**) SHROOM3-3M in nonprogressors (ΔCADI<2) and progressors (ΔCADI≥2). (**A**–**F**) SHROOM3-3M values are presented as log-transformed fluorescence relative to normal preperfusion biopsies. Data represent individual allograft samples (dots) and regression line of the correlation (**A**,**B**, **D**, and **E**) or mean ± SEM (**C** and **F**). *$P < 0.05$, unpaired *t* test.

The A allele of rs17319721 enhances SHROOM3 expression through TCF7L2-mediated transcriptional activation. We next investigated the mechanism of the increased *SHROOM3* transcript levels observed with the presence of the risk allele in the donor. Examination of the intronic region of the rs17319721 *SHROOM3* SNP revealed a potential consensus binding sequence for the TCF/LEF high-mobility group domain family of transcription factors, which have the consensus binding sequence of 5′-(A/T)(A/T)CAAAG-3′. The rs17319721 SNP localizes to the penultimate nucleotide of this consensus binding sequence. Proteins of the TCF/LEF family are involved in canonical β-catenin/TCF/LEF–dependent Wnt signaling (13, 14). Under the basal condition, TCF/LEF bind to the consensus binding site and act as repressors of gene transcription by recruiting corepressors such as Groucho and CtBP. In the presence of Wnt ligand, β-catenin accumulates in the cytoplasm and nucleus. β-Catenin binding to the TCF/LEF–DNA complex promotes recruitment of coactivators, leading to activation of gene transcription. As the A allele of rs17319721 was linked to higher allograft *SHROOM3* expression compared with the G allele, we reasoned that single nucleotide variation of the TCF/LEF consensus binding sequence at rs17319721 could dictate TCF/LEF binding and/or its transcriptional activity to influence *SHROOM3* expression. Of the 4 TCF/LEF genes — *TCF1*, *TCF3*, *TCF7L2*, and *LEF* — only *TCF7L2* was markedly upregulated in allografts of the highest versus the lowest quartile of SHROOM3-3M ($\log_2$ $r = 0.74$, $P < 0.0001$; Supplemental Table 5). We found that knockdown of *TCF7L2* in HK2 cells (tubular cell line) markedly diminished SHROOM3 protein levels (Figure 3A), which suggests that *SHROOM3* expression is indeed TCF7L2 dependent. While overexpression of a WT *TCF7L2* gene construct (WT-TCF7L2) did not increase SHROOM3 protein levels in HK2 cells, which were of the A/A genotype, overexpression of a dominant-negative mutant of *TCF7L2* that lacks the N-terminal β-catenin binding domain (DN-TCF7L2) markedly decreased SHROOM3 protein expression compared with both GFP- and WT-TCF7L2–transfected cells (Figure 3B). The observed lack of response in SHROOM3 protein expression with WT-TCF7L2 overexpression is in line with TCF7L2's role as a corepressor under the basal condition.

To confirm the interaction of TCF7L2 with the putative consensus binding site within the first intron of *SHROOM3*, we performed EMSA. We generated 2 variants of a 36-bp double-stranded DNA probe, containing the putative TCF/LEF binding sequence derived from the intronic sequence of *SHROOM3*, to contain either the A or the G allele (A probe and G probe, respectively; Supplemental Table 6). Under the basal condition, the A probe was bound to TCF7L2, either alone or in a complex with β-catenin (Figure 3C,

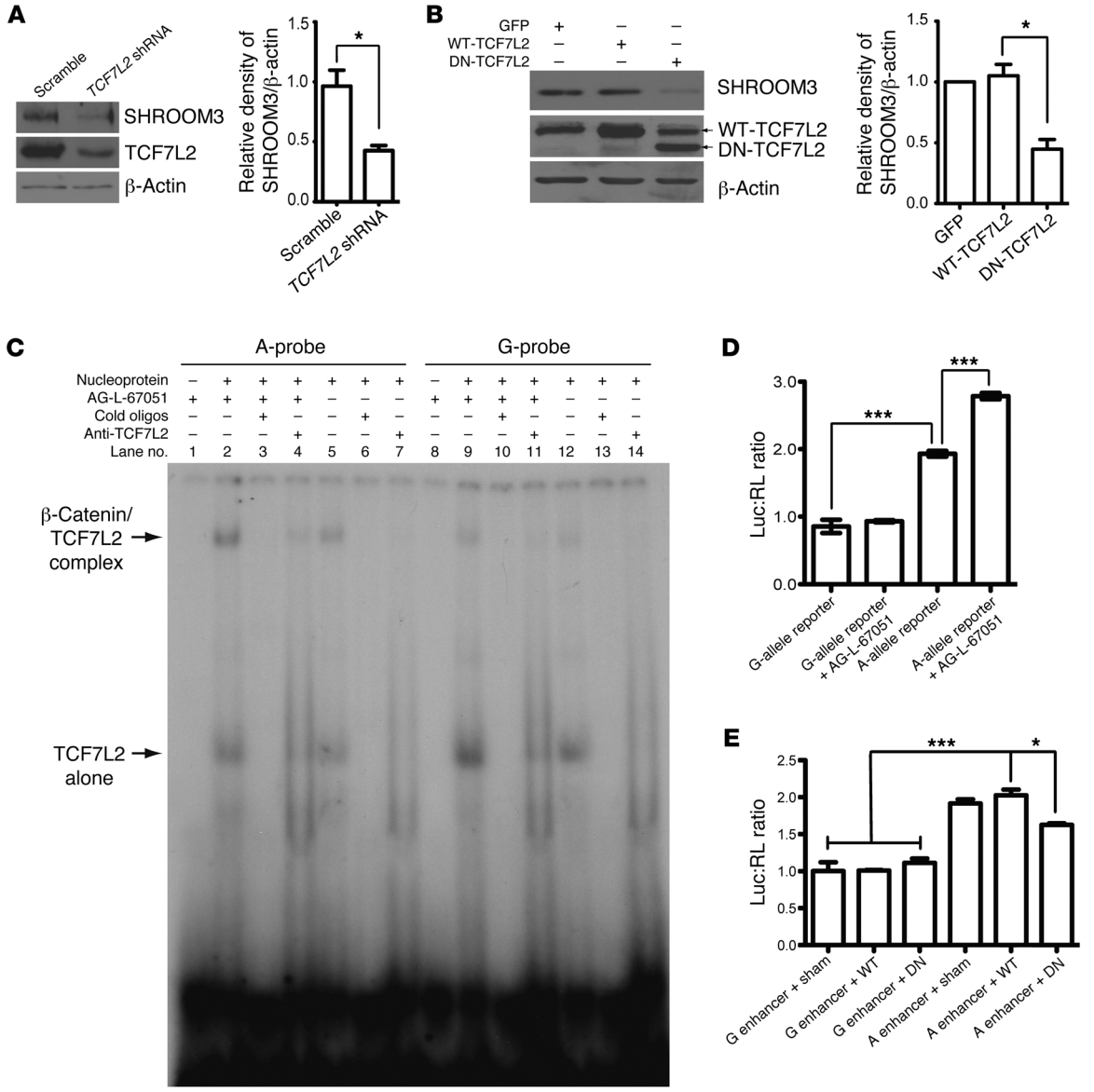

Figure 3. The A allele of rs17319721 enhances *SHROOM3* expression through β-catenin/TCF7L2–mediated transcriptional activation. (**A** and **B**) Representative WBs of (**A**) SHROOM3 and TCF7L2 in HK2 cells infected with a scrambled or *TCF7L2*-specific GIPZ lentiviral shRNA, and of (**B**) SHROOM3 and TCF7L2 in HK2 cells transfected with GFP control, WT-TCF7L2, or DN-TCF7L2 expression constructs. DN-TCF7L2 lacked the β-catenin–binding domain and migrated further than WT-TCF7L2 on the gel (arrows). Relative density of SHROOM3 normalized to β-actin is also shown (n = 3). (**C**) Representative gel of EMSA of nucleoprotein from HEK-293 cells. Cells were cultured in the presence (lanes 1–4 and 8–11) or absence (lanes 4–7 and 12–14) of the Wnt agonist AG-L-67051 (100 nM). Nucleoprotein (4 μg) was incubated with 36-bp oligonucleotide probes containing either A or G allele sequences. Lanes 1–7, A probe; lanes 8–14, G probe. Supershifting with anti-TCF7L2 antibody prior to incubation with probes was performed (lanes 7–14). The higher band (top arrow) corresponds to a protein/DNA complex containing β-catenin and TCF7L2; the lower band (bottom arrow) corresponds to a protein/DNA complex with TCF7L2 only (n = 3). (**D** and **E**) Promoter-enhancer-reporter constructs with 3-kb human SHROOM3 promoter and A or G allele enhancer sequences (24 bp) were transfected into HEK-293T cells. (**D**) Luciferase/renilla ratio (Luc:RL) of A and G allele reporter activity (with and without AG-L-67051). (**E**) Luciferase/renilla ratio in HEK-293T cells cotransfected with either reporter plasmid and WT-TCF7L2, DN-TCF7L2, or sham plasmids (pcDNA3.1) and cultured in the presence of AG-L-67051 (n = 3). Data represent mean ± SEM. $^*P < 0.05$, $^{***}P < 0.0001$, unpaired t test (**A** and **B**); ANOVA with post-test Bonferroni comparison (**D** and **E**).

lane 5, arrows). In contrast, the G probe was bound mostly to TCF7L2 alone (Figure 3C, lane 12). β-catenin binding to TCF7L2-DNA complex represents transcriptional activation. Treatment with the Wnt agonist AG-L-67051 increased binding of both the TCF7L2/β-catenin complex and TCF7L2 alone to the A probe, but not the G probe (Figure 3C, lanes 2 and 9). AG-L-67051 treatment had no marked effect on binding of TCF7L2 alone to either probe (Figure 3C, lanes 2, 5, 9 and 12). Taken together, these findings confirmed that (a) TCF7L2 binds to the putative consensus binding sequence within *SHROOM3*'s intron, (b) the A allele preferentially binds the TCF7L2/β-catenin complex, and (c) Wnt agonist treatment increases TCF7L2/β-catenin complex binding to the A allele, but not the G allele. Incubation with specific antibodies and competition with an excess of cold oligonucleotides abolished probe-

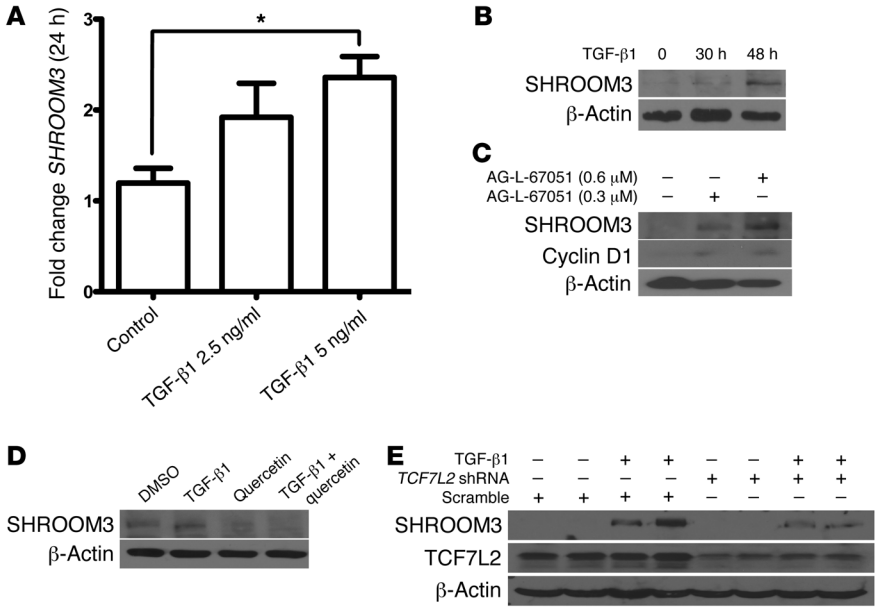

Figure 4. TGF-β1 increases *SHROOM3* in a β-catenin/TCF7L2–dependent manner. (**A**) *SHROOM3* mRNA transcript levels (normalized to *GAPDH*) in PRCECs treated for 24 hours with TGF-β1 (2.5 and 5 ng/ml) relative to cells without TGF-β1 treatment. Values are mean ± SEM ($n = 3$). *$P < 0.05$, ANOVA with post-test Bonferroni comparison. (**B** and **C**) Representative WBs of (**B**) SHROOM3 and β-actin in PRCECs treated with TGF-β1 (5 ng/ml) for 30 and 48 hours and (**C**) SHROOM3, cyclin D1, and β-actin in HK2 cells treated with AG-L-67051 (0.3 or 0.6 μM) for 48 hours ($n = 3$ sets each). (**D**) HK2 tubular cells were treated with and without TGF-β1 (5 ng/ml) in the presence or absence of the β-catenin inhibitor quercetin (10 μM). Shown are representative WBs of SHROOM3 and β-actin at 30 hours ($n = 3$ independent sets). (**E**) HK2 cells (cultured in 6-cm dishes), infected with lentiviral constructs containing either scrambled or TCF7L2 shRNA, were treated with TGF-β1 (5 ng/ml) for 48 hours. Shown are representative WBs of SHROOM3, TCF7L2, and β-actin from duplicate experiments ($n = 3$ sets).

nucleoprotein interactions (Figure 3C, lanes 4, 6, 7, 11, 13, and 14), demonstrating the identity of the TCF7L2/β-catenin complex and its specificity of binding to the synthetic oligonucleotide.

To examine whether transcriptional complex-DNA binding documented by EMSA translates into enhanced SHROOM3 expression, we performed reporter assays using promoter-enhancer luciferase reporter constructs that consisted of a 24-bp sequence from the first intron of *SHROOM3* containing either the A allele or the G allele of rs17319721 fused with a 3-kb *SHROOM3* promoter sequence (Supplemental Table 6 and Supplemental Figure 3). Under the basal condition (i.e., without AG-L-67051 treatment), A allele reporter activity was more than 2-fold higher than that of the G allele. Treatment with AG-L-67051 further increased the activity of the A allele reporter, but had no effect on that of G allele reporter–transfected cells (Figure 3D). Overexpression of DN-TCF7L2 (lacking the β-catenin–binding domain) significantly reduced AG-L-67051–induced activity from the A allele reporter compared with overexpression of WT-TCF7L2, whereas neither affected G allele reporter activity (Figure 3E). These findings were consistent with our EMSA observations, in which the G probe was not noticeably associated with the active, β-catenin–associated form of TCF7L2. Taken together, our results suggest that AG-L-67051–induced activation of the A allele reporter is dependent on interaction of TCF7L2 with β-catenin.

SHROOM3 expression is regulated by TGF-β1 in a Wnt/β-catenin/TCF7L2–dependent manner. Given that *SHROOM3* is regulated by TGF-β1 in HK2 cells (15), and TGF-β1 is a key growth factor mediating renal injury and fibrosis (16, 17), we sought to further characterize TGF-β1–mediated regulation of *SHROOM3* expression. Since immunostaining showed the localization of SHROOM3 to be predominantly in the tubular compartment of healthy controls, we performed in vitro studies on primary renal cortical epithelial cells (PRCECs) and tubular cell lines (HK2) (Supplemental Figure 4). TGF-β1 treatment of PRCECs increased both mRNA and protein expression of SHROOM3 (Figure 4, A and B). AG-L-67051 also increased SHROOM3 in a dose-dependent manner in HK2 cells of A/A genotype (Figure 4C). Analysis of the *SHROOM3* promoter sequence — up to –10 kb from the transcriptional start site — using a transcription factor binding motif prediction program (TRANSFAC) did not reveal any SMAD-binding sequence, which suggests that the TGF-β1–induced increase in *SHROOM3* expression is not due to canonical TGF-β1/SMAD signaling. As TGF-β1 is known to crosstalk with the Wnt/β-catenin/TCF pathway, and Wnt agonist treatment and TCF7L2 mediated *SHROOM3* expression, we tested whether TGF-β1–induced *SHROOM3* expression is dependent on β-catenin/TCF interaction. We found that quercetin, a β-catenin inhibitor, substantially abrogated TGF-β1–induced SHROOM3 protein (Figure 4D). Furthermore, HK2 cells with *TCF7L2* knockdown showed markedly less upregulation of SHROOM3 upon treatment with TGF-β1 (Figure 4E). These data confirmed that TGF-β1–induced *SHROOM3* expression is β-catenin/TCF7L2 dependent in renal tubular cells.

SHROOM3 facilitates canonical TGF-β1/SMAD3 signaling and profibrotic gene expression in vitro. Next, we investigated whether *SHROOM3* in turn has any effect on TGF-β1–mediated profibrotic gene expression, a well-characterized driver of kidney fibrosis in CKD as well as CAN (16, 17). α1 Collagen (*COL1A1*) is a key TGF-β1–induced profibrotic gene product. First, we compared expression of *COL1A1* in PRCECs with or without *SHROOM3* overexpression, treated with TGF-β1 or vehicle. Overexpression of *SHROOM3* was confirmed by quantitative RT-PCR and Western blotting (WB) (Supplemental Figure 5, A and B). Expression of *COL1A1* was increased by TGF-β1 treatment alone as well as by *SHROOM3* overexpression (Figure 5A). *SHROOM3*-overexpressed PRCECs also displayed more prominent F-actin bundles compared with cells without *SHROOM3* overexpression (Supplemental Figure 5C), consistent with SHROOM3's function as a F-actin–binding protein that regulates its subcellular distribution. TGF-β1–induced *COL1A1* expression was further increased in cells with *SHROOM3* overexpression compared with TGF-β1–treated cells without *SHROOM3* overexpression. To further characterize how SHROOM3 facilitates TGF-β1 signaling, we investigated the phosphorylation of SMAD3,

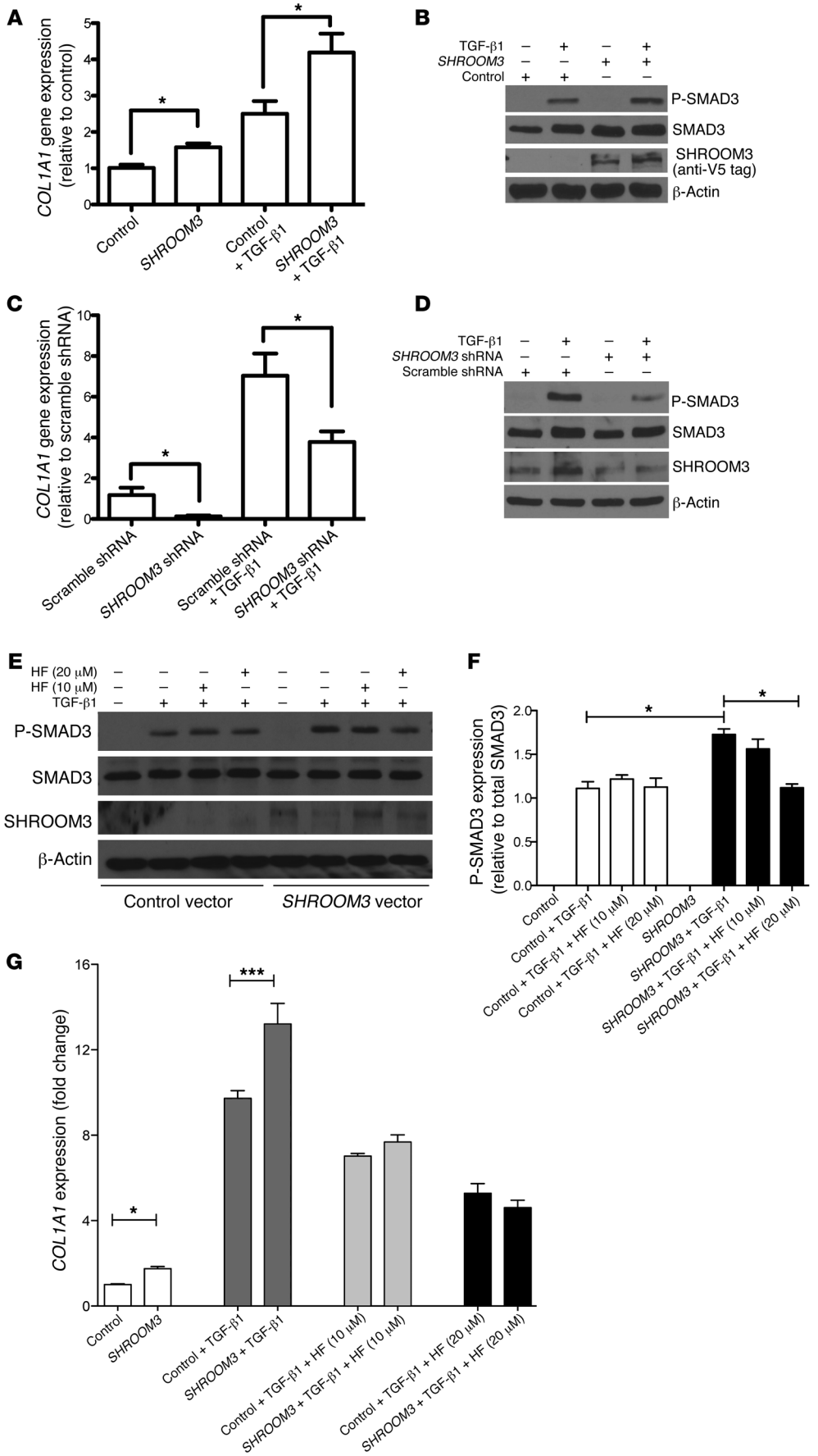

Figure 5. *SHROOM3* facilitates canonical TGF-β1/SMAD3 signaling and profibrotic gene expression in vitro. (**A** and **B**) Control- and *SHROOM3*-transfected PRCECs were treated or not with TGF-β1 (5 ng/ml). (**A**) Relative *COL1A1* transcript levels, by RT-PCR (normalized to *GAPDH*), after 24 hours of TGF-β1 treatment (n = 4 sets). (**B**) WBs of phospho- and total SMAD3, SHROOM3 (anti-V5 tag), and β-actin at 30 minutes of TGF-β1 treatment. (**C** and **D**) Lentiviral shRNA–mediated knockdown of *SHROOM3* was performed in PRCECs. (**C**) Relative *COL1A1* transcript levels, by RT-PCR (normalized to *GAPDH*), after 24 hours of TGF-β1 treatment. (**D**) Cells were treated with TGF-β1 for 30 minutes. Shown are WBs of phospho-SMAD3, SMAD3, SHROOM3, and β-actin of a representative experiment of 4. (**E**–**G**) PRCECs transfected with *SHROOM3* or control were treated with 10 or 20 μM HF for 12 hours in serum-starved medium. (**E**) Phosphorylation of SMAD3 was assayed in lysates after 30 minutes of TGF-β1 treatment. Representative WB of phospho-SMAD3, SMAD3, SHROOM3, and β-actin is shown. (**F**) Densitometry of relative phospho-SMAD3 (n = 3 sets). (**G**) 24 hours after transfection, PRCECs were continuously treated with HF for 24 hours in serum-starved medium. TGF-β1 or vehicle was added for the final 12 hours. Relative *COL1A1* mRNA, by RT-PCR (normalized to *GAPDH*), was determined after 48 hours of transfection (n = 3). (**A**, **C**, **F**, and **G**) Values are mean ± SEM. $^{*}P < 0.05$; $^{**}P < 0.001$; $^{***}P < 0.0001$, ANOVA with post-test Bonferroni comparisons.

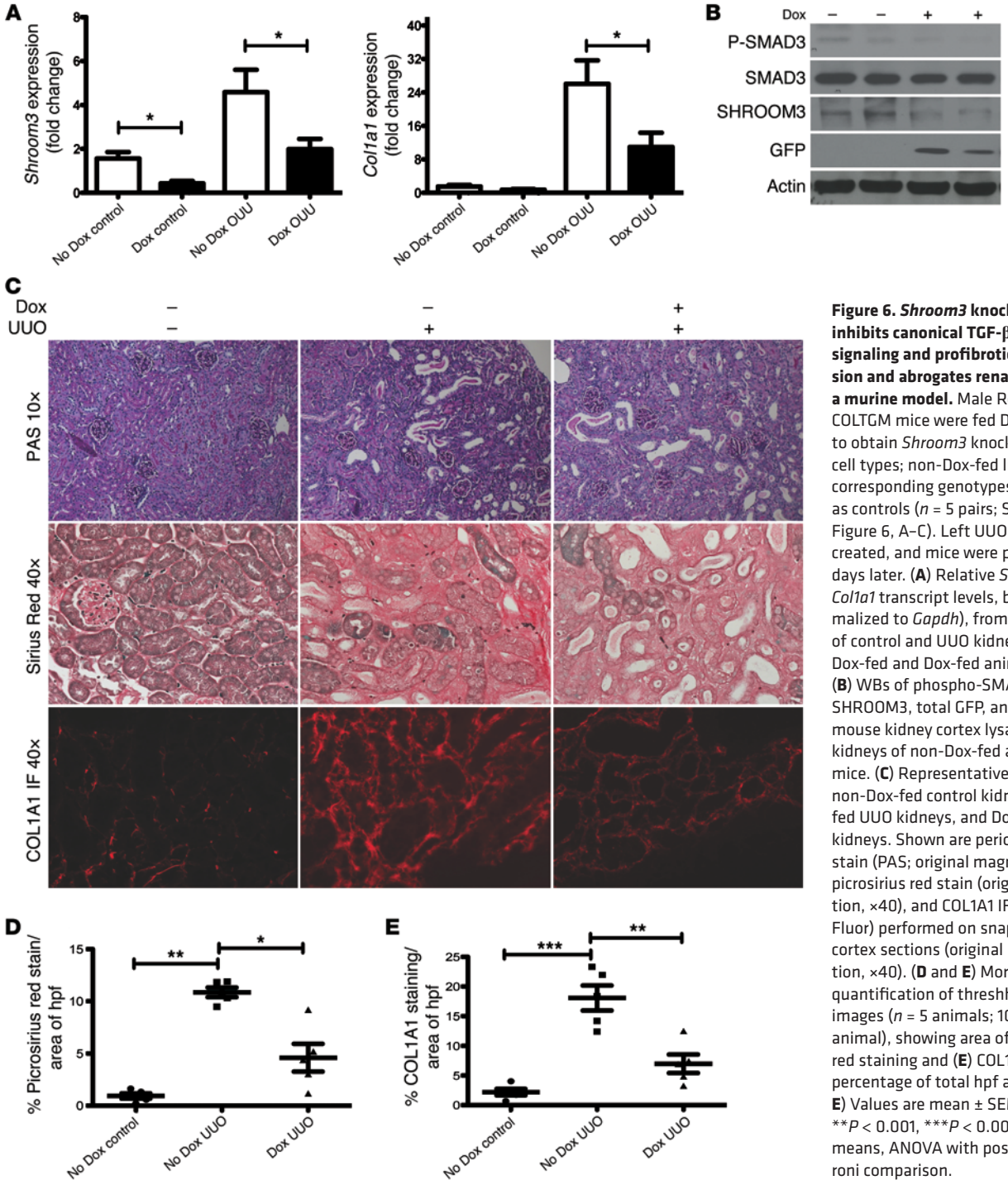

Figure 6. *Shroom3* knockdown in vivo inhibits canonical TGF-β1/SMAD3 signaling and profibrotic gene expression and abrogates renal fibrosis in a murine model. Male Rosa-RTTA/COLTGM mice were fed Dox for 3 weeks to obtain *Shroom3* knockdown in all cell types; non-Dox-fed littermates of corresponding genotypes were used as controls (n = 5 pairs; Supplemental Figure 6, A–C). Left UUO was surgically created, and mice were perfused 10 days later. (**A**) Relative *Shroom3* and *Col1a1* transcript levels, by RT-PCR (normalized to *Gapdh*), from whole cortices of control and UUO kidneys of non-Dox-fed and Dox-fed animals (n = 5). (**B**) WBs of phospho-SMAD3, SMAD3, SHROOM3, total GFP, and β-actin from mouse kidney cortex lysates from UUO kidneys of non-Dox-fed and Dox-fed mice. (**C**) Representative images from non-Dox-fed control kidneys, non-Dox-fed UUO kidneys, and Dox-fed UUO kidneys. Shown are periodic acid–Schiff stain (PAS; original magnification, ×10), picrosirius red stain (original magnification, ×40), and COL1A1 IF (TRITC–Alexa Fluor) performed on snap-frozen kidney cortex sections (original magnification, ×40). (**D** and **E**) Morphometric quantification of threshholded ×40 images (n = 5 animals; 10 random hpfs/animal), showing area of (**D**) picrosirius red staining and (**E**) COL1A1 IF as a percentage of total hpf area. (**A**, **D**, and **E**) Values are mean ± SEM. $^*P \le 0.05$, $^{**}P < 0.001$, $^{***}P < 0.0001$ between means, ANOVA with post-test Bonferroni comparison.

which is indicative of activation of canonical TGF-β1/SMAD signaling. Cells with and without *SHROOM3* overexpression were treated with either TGF-β1 or vehicle. Phosphorylation of SMAD3 in TGF-β1–treated cells was enhanced by *SHROOM3* overexpression compared with control vector–transfected cells (Figure 5B). Next, we sought to determine whether TGF-β1–induced profibrotic gene expression is dependent on SHROOM3. *SHROOM3* knockdown in PRCECs significantly reduced *COL1A1* mRNA transcript levels, and TGF-β1–induced expression of *COL1A1* was also significantly attenuated in *SHROOM3* knockdown cells compared with cells transduced with the empty lentivector (Figure 5C). Phosphorylation of SMAD3 in *SHROOM3* knockdown cells was substantially reduced 30 minutes after TGF-β1 stimulation compared with cells without *SHROOM3* knockdown (Figure 5D). The interaction between the ASD-2 domain of *SHROOM3* and RHO kinases (ROCK-1 and ROCK-2) has been previously described (18). Facilitation of SMAD3 phosphorylation by ROCK has also been noted (19). To examine whether the mechanism of TGF-β1 signaling facilitation by *SHROOM3* is mediated by ROCK, we treated *SHROOM3*-transfected cells with the ROCK inhibitor hydroxyfasudil (HF). The facilitation of phospho-SMAD3 by *SHROOM3* in response to TGF-β1 was inhibited by HF (Figure 5, E and F). *COL1A1* over-

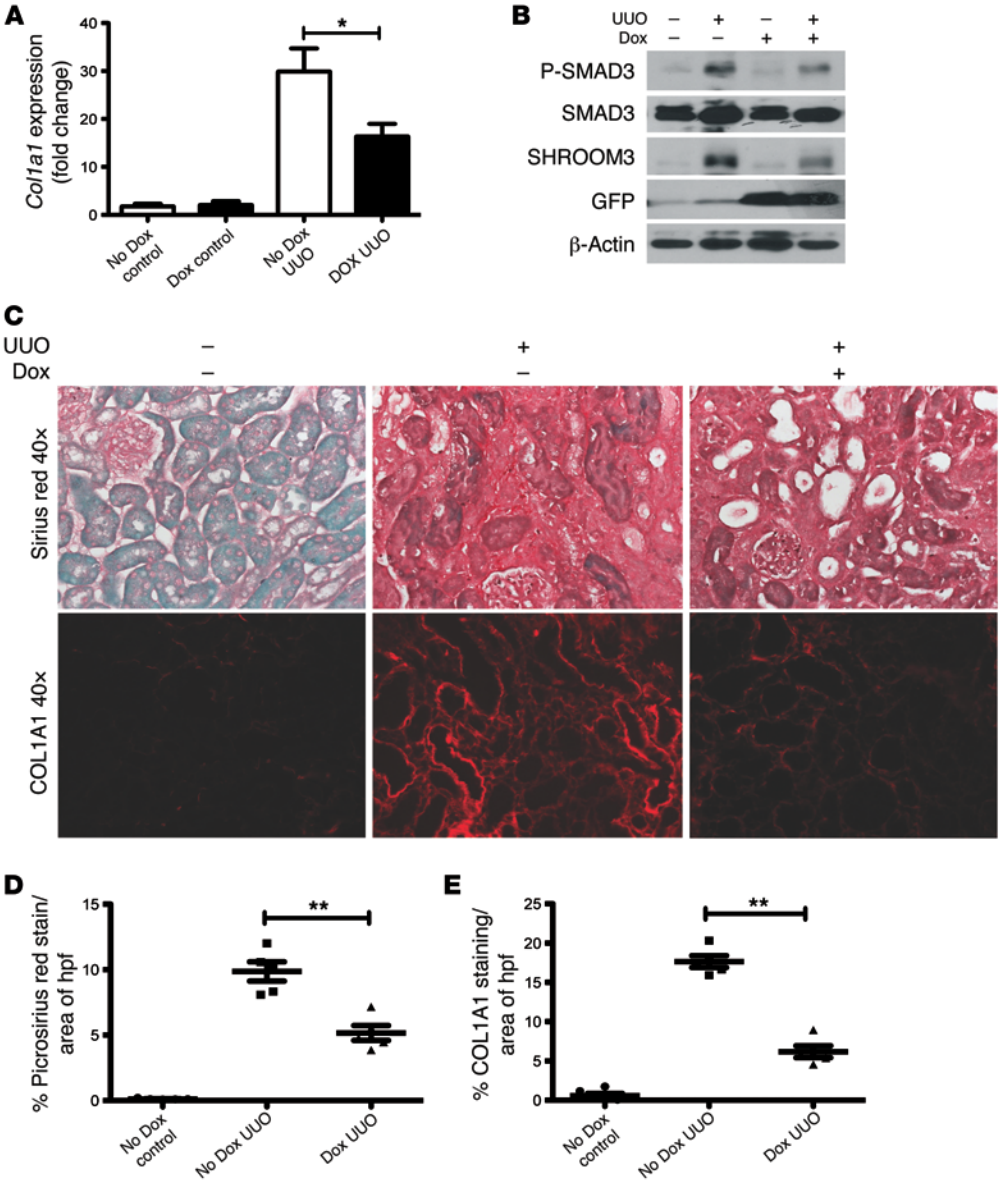

Figure 7. Selective *Shroom3* knockdown in tubular cells inhibits canonical TGF-β1/SMAD3 signaling and profibrotic gene expression and abrogates renal fibrosis in a murine model. To achieve *Shroom3* knockdown exclusively in tubular cells, PAX8-RTTA/COLTGM mice were fed Dox for 3 weeks; non-Dox-fed littermates of the corresponding genotype were used as controls. Dox feeding of PAX8-RTTA/COLTGM mice induced *Shroom3* knockdown and GFP production in tubular cells (Supplemental Figure 7). Left UUO was surgically created, and mice were perfused 10 days later. (**A**) Relative *Col1a1* mRNA, by RT-PCR (normalized to *Gapdh*). (**B**) Representative WBs for phospho-SMAD3, SMAD3, Shroom3, total GFP, and β-actin between Dox-fed and non-Dox-fed PAX8-RTTA mice. (**C**–**E**) Representative microphotographs (**C**; original magnification, ×40) from kidney sections of picrosirius red staining and COL1A1 IF, and corresponding morphometric quantifications for (**D**) Sirius red and (**E**) COL1A1 (n = 5 animals; 10 random hpfs/animal). Data are mean ± SEM. $^{*}P \leq 0.05$, $^{**}P < 0.001$ between means, ANOVA with post-test Bonferroni comparison.

production by *SHROOM3* was also reduced by HF, as assessed by RT-PCR (Figure 5G). Taken together, these results suggest that SHROOM3 enhances the TGF-β1/SMAD3–induced profibrotic signaling pathway in kidney tubular cells. Furthermore, expression of profibrotic genes including *CTGF*, *Vimentin*, and *Collagen IV* (downstream targets of TGF-β1/SMAD3 signaling) were significantly upregulated in allografts within the highest quartile of *SHROOM3* expression (Supplemental Table 5). In view of this association, and to delineate whether the effect of SHROOM3-3M on CADI-12 was due to its relationship with CTGF, we added CTGF expression along with SHROOM3-3M as a covariate for CADI-12 in the multivariate model. CTGF levels as a covariate had no effect on CADI-12≥2 outcome, no effect on OR estimates, and minimal effect on *P* values observed using SHROOM3-3M as predictor (Supplemental Table 7).

SHROOM3 facilitates canonical TGF-β1/SMAD3 signaling and profibrotic gene expression in a murine model in vivo. We then examined the effect of shRNA-mediated *Shroom3* knockdown on TGF-β1/SMAD3 signaling and renal fibrosis in a doxycycline-inducible (Dox-inducible) mouse strain (20). In our model, RTTA elements were linked to the universal ROSAm26 promoter for RTTA expression in all cell types (referred to herein as Rosa-RTTA). After in vitro validation, a *Shroom3*-specific shRNA was linked to Dox-RTTA–responsive elements and positioned 3′ to the *Col1a1* gene (Supplemental Figure 6, A and B). To study the development of renal interstitial fibrosis, we performed unilateral ureteric obstruction surgery (UUO) on 8- to 10-week-old animals (n = 5). Dox feeding to induce *Shroom3* knockdown in the Rosa-RTTA mice was initiated 3 weeks prior to UUO surgery and continued until sacrifice 10 days after the procedure (Supplemental Figure 6C). Non-Dox-fed littermates with UUO were used as controls. *Shroom3* knockdown was confirmed by RT-PCR and WB in renal cortical lysates (Figure 6, A and B). Dox-fed animals showed substantially inhibited phosphorylation of SMAD3 in UUO kidneys by WB (Figure 6B). *Tgfb1* mRNA levels were similar between cortices of Dox-UUO and non-Dox-UUO kidneys (Supplemen-

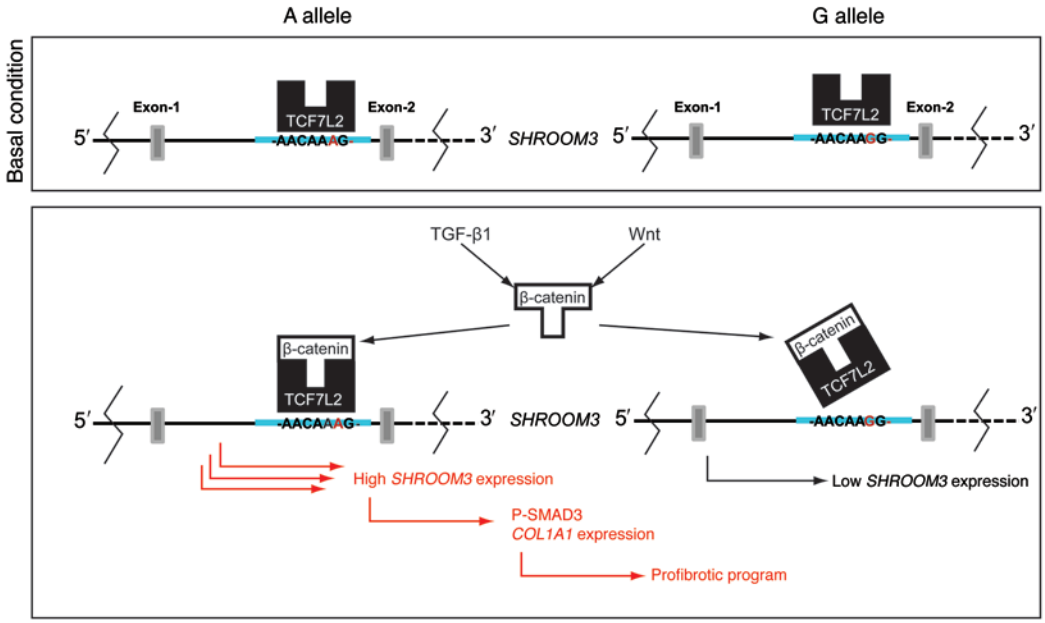

Figure 8. TCF7L2-dependent enhancer function of the A allele of rs17319721 that culminates in renal fibrosis. In the basal condition, TCF7L2 binds the intronic sequence of *SHROOM3* containing either A or G alleles at rs17319721 and is a transcriptional repressor. Signaling of the profibrotic mediators TGF-β1 and Wnt leads to cytoplasmic and nuclear β-catenin accumulation. When β-catenin binds TCF7L2, this transcriptionally active complex preferentially binds the A allele sequence, enhancing *SHROOM3* transcription. SHROOM3 facilitates canonical TGF-β1 signaling and profibrotic program, promoting renal interstitial fibrosis in CAN and CKD.

tal Figure 6D), which suggested that difference in TGF-β1 levels was not responsible for difference in SMAD3 phosphorylation. COL1A1 production in UUO kidneys was inhibited with *Shroom3* knockdown, as assessed by RT-PCR of kidney lysates and by immunofluorescence (IF) in tissue (Figure 6, A, C, and E). Renal interstitial fibrosis, measured by picrosirius red staining, was significantly abrogated with *Shroom3* knockdown (Figure 6, C and D).

In the Rosa-RTTA mice with induced *Shroom3* knockdown, the *Shroom3* knockdown was global and occurred in all tissues and cell types. To specifically study the effects of *Shroom3* knockdown in renal tubular cells, we adapted our hairpin to PAX8-RTTA animals for shRNA and GFP production in tubular cells upon Dox feeding (Supplemental Figure 7). As with global *Shroom3* knockdown, tubular cell–specific knockdown of *Shroom3* in these PAX8-RTTA mice reduced phosphorylation of SMAD3, mRNA and protein expression of COL1A1, and renal interstitial fibrosis ($n = 5$ sets; Figure 7, A–E). These data indicate that the major effect of *Shroom3* knockdown on TGF-β1 signaling and renal fibrosis can be isolated to tubular cells.

These findings validated the role of tubular cell SHROOM3 in canonical TGF-β1 signaling and were in keeping with our in vitro and human allograft observations. Taken together, our present data suggest an increased profibrotic program in the presence of the enhancer function of the risk allele and/or increased SHROOM3 expression (Figure 8).

Discussion

Arising from diverse causes, CAN is the main cause for allograft failure and renal replacement therapy (3, 21). Modern immunosuppressive strategies have had significant effects on short-term allograft outcomes, with much less improvement in long-term outcomes (22, 23). Here, we identified *SHROOM3* as a novel candidate gene whose allograft expression preceded and correlated with the decline of renal function, while the presence of the risk allele of a CKD-associated intronic *SHROOM3* SNP, rs17319721, in the donor correlated with TIF and CAN at 12 months. We delineated the β-catenin/TCF7L2–dependent enhancer function of this risk allele at rs17319721 on *SHROOM3* expression and showed that SHROOM3 enhanced TGF-β1/SMAD3 signaling to increase profibrotic gene expression. We also demonstrated that *Shroom3* knockdown abrogated renal interstitial fibrosis in a murine UUO model, an effect that could be isolated as arising from tubular cells, suggestive of a common role for SHROOM3 in CKD and CAN.

TIF is a common histological endpoint for CAN and CKD. Consequently, genes linked to fibrogenesis and extracellular matrix production, specifically related to TGF-β1 signaling, have emerged in gene expression studies of CAN and CKD as being differentially regulated (24–27). The *SHROOM3* SNP has been linked to incident and prevalent CKD (8–10). However, both the role of the SNP and SHROOM3's function and relationship to eGFR loss and CKD are unknown. Our in vivo and in vitro data suggested that SHROOM3 enhances canonical TGF-β1 signaling and increases *COL1A1* in renal cortical cells. We showed that this effect was mediated in part by ROCK facilitation. We also showed that TGF-β1 regulated *SHROOM3* in a β-catenin/TCF7L2–dependent manner. Increased *SHROOM3*, in turn, enhanced TGF-β1–mediated profibrotic response in renal epithelial cells (Figure 6), indicative of a positive feedback loop among TGF-β1, Wnt/β-catenin signaling, and *SHROOM3*. TCF7L2 is downstream of the Wnt/β-catenin signaling pathway, which has been independently linked to kidney fibrosis (28). Furthermore, the TGF-β1 signaling cascade is known to interact with and facilitate Wnt signaling by promoting

accumulation of nuclear β-catenin in renal tubular epithelial cells (29, 30). Our present findings suggest that SHROOM3 may toggle on both of these key profibrotic pathways.

A summary of published GWAS studies concluded that approximately 80% of trait-associated SNPs are located in noncoding regions (31). Results from the Encyclopedia of DNA elements (ENCODE) consortium have attributed important regulatory functions to these noncoding intronic loci within the human genome (32–34). To date, several publications have associated the intronic rs17319721 in *SHROOM3* with the development of CKD (8–10). From our biopsy data, having 1 or 2 copies of the risk allele, A, in the allograft appeared to significantly increase *SHROOM3* transcript levels in biopsy tissue. However, we were unable to identify a consistent association between SHROOM3-3M and recipient genotype at rs17319721 or the presence of acute rejection (data not shown), which suggests that the observed relationship between *SHROOM3* expression and indices of allograft function could not be attributed to recipient cells infiltrating the allograft. The preeminent role of donor-derived or resident kidney cell SHROOM3 in renal fibrosis was further implied by the observed effects in vivo with tubular cell–specific *Shroom3* knockdown.

It has been observed that complex trait-associated SNPs are more likely to be expression quantitative trait loci (eQTLs) rather than minor allele frequency–matched SNPs (35). Our present study describes a CKD-related SNP, rs17319721, as an intronic eQTL. From the latest releases of HAPMAP and 1000 Genomes data, we simultaneously verified that the 3 other SNPs in complete linkage with rs17319721 were not in chromatin regions annotated as promoters, enhancers, DNASe-I hypersensitivity regions, or sequences serving as consensus binding sites for known transcription factors, while rs17319721 lies within a DNASe-I hypersensitivity region and conforms to TCF/LEF binding sequence (36–38). We experimentally demonstrated that rs17319721 functioned as a *cis*-acting element with specific TCF7L2-dependent enhancer function promoting *SHROOM3* expression. While both variants of the SNP bound free TCF7L2 with equal affinity, the transcriptionally active, β-catenin–bound TCF7L2 preferentially associated with the A allele. Taken together, our data strongly suggest that the association between the A allele and CKD in prior GWAS studies may be explained in part by increased Wnt/β-catenin–mediated *SHROOM3* expression that facilitates TGF-β1–mediated profibrotic programs (Figure 8). This is supported by our finding that recipients of allografts that had 1 or 2 copies of the risk allele had a higher likelihood of developing significant allograft injury (i.e., CADI-12≥2, which has been correlated with adverse graft outcomes; ref. 6). Therefore, our study also identifies a donor polymorphism that predisposes the recipient to CAN. In addition, when A/A donor genotype kidneys were compared with G/G donors, the only significantly differentially upregulated gene in the A/A group from our microarray data was *CTGF*, which is a key facilitator of TGF-β1 action in various fibrotic models (39, 40). Functional genomic studies such as ours that integrate static genomic information (i.e., disease-associated SNPs) with dynamic gene transcription and protein-protein interactions offer insight into the biologic relevance of widely encountered genetic variations that could serve particular pathogenic roles in disease states.

Distinct gene signatures have emerged from prior transcriptional studies on CAN (41). Development of molecular targets for therapeutics have been impeded by large gene panel sizes, small sample sizes, use of for-cause biopsies, heterogeneity of gene chip assay used, and low fidelity of prearray amplification techniques (42, 43). Importantly, specific mechanistic data implicating the numerous genes identified in CAN development and progression are lacking. Here we used whole-exon gene chip array (~4 probes/exon, ~40 probes/gene) to profile gene expression pattern from 3-month protocol biopsies. Our parent study, GoCAR, represents the largest prospective protocol allograft expression data to date. SHROOM3-3M in the present study retained its significance when analyzed alone. Importantly, mean *SHROOM3* transcript levels in patients categorized as CAN progressors were significantly higher than in nonprogressors with relatively stable renal histological features, lending further support to a role for SHROOM3 in CAN progression.

In univariate and multivariate analyses, the association between *SHROOM3* and eGFR/CADI was significant in Caucasian donor kidney recipients, but not in non-Caucasian donor allografts. The allelic prevalence of the A allele was significantly higher in Caucasians compared with non-Caucasians in our cohort. Prior GWAS studies that identified the *SHROOM3* SNP involved Caucasian-predominant cohorts (8–10). In a study to identify susceptibility loci for proteinuria, which is pathognomonic of renal injury, the rs17319721 SNP was associated with both eGFR and proteinuria outcomes in Caucasians, but not in African-Americans (44). These results are analogous to the lack of association between *SHROOM3* expression and eGFR/CADI in non-Caucasian allografts observed here in the GoCAR cohort.

Our current study has limitations. Not all the patients in the 3-month microarray had biopsies for outcome assessment at 12 months. However, our sample size of 101 patients was still robust compared with prior transcriptional studies in allograft recipients (41, 45, 46). Only 32 patients had sufficient quality RNA for RT-PCR validation after microarray, although robust concordance was present within these samples. Finally, in spite of the statistically significant difference in mean SHROOM3-3M between progressors and nonprogressors, there remained substantial overlap between these groups, precluding the use of a single value of SHROOM3-3M as a biomarker from our current study data. However, the donor rs17319721 genotype may hold promise as a marker to predict allografts that are at risk for CAN. Moreover, when added to composite models that may include other clinical/demographic variables, SHROOM3-3M could enhance the ability to predict allografts that sustain progressive histological and functional decline, especially among Caucasian donor allografts. Both these findings need to be further validated in large transplant cohorts.

In summary, we have identified *SHROOM3* as a novel candidate gene whose expression in the renal allograft antedates and correlates with the decline of renal function in CAN. We described the CKD-associated SNP in SHROOM3, rs17319721, as an eQTL. Furthermore, we demonstrated that the risk allele at this intronic *cis*-eQTL had a specific TCF7L2-dependent enhancer function promoting *SHROOM3* expression. The risk genotype in the donor corresponded to increased risk of CAN through higher allograft *SHROOM3* levels. Finally, we found that SHROOM3 enhanced canonical TGF-β1 signaling and *COL1A1* expression in renal tubular cells and demonstrated abrogated renal interstitial fibrosis in

vivo with *Shroom3* knockdown. Thus, SHROOM3 may represent a potential therapeutic target to reduce the progression of TIF in patients with CKD or CAN.

Methods

GoCAR study. Real-time, ultrasound-guided, renal allograft biopsies were obtained 0, 3, 12, and 24 months after transplant at 3 of 5 clinical sites. 2 biopsy cores were taken when possible using 18G spring-loaded biopsy needles. If a single core was obtained, preference was given to RNA extraction (ALLprep kit; QIAGEN) at the 3-month visit and to histological analysis at the 12-month visit. Tissue for gene expression studies was stored immediately in RNA-later and shipped at –20°C to the genomics core facility at Icahn School of Medicine at Mount Sinai. Patients were followed per regular posttransplant routine at the respective centers. Gene expression microarray analysis was performed on RNA extracted from allograft biopsies at 3 months on 159 patients (Affymetrix Human Exon-1 Chip). Microarrays were read using GeneArray Scanner (Affymetrix) and analyzed with GeneChip Operating Software (version 1.4.0, Affymetrix). The intensity data at gene level was extracted and summarized with RMA algorithm, and data quality was assessed using Affymetrix Expression Console (Affymetrix Inc.). The Affymetrix control probesets or the probesets with low intensity across all samples were excluded from downstream analysis. The batch effect due to the difference of 2 amplification and labeling protocols applied in this study was adjusted using the ComBat R package. Measurements were expressed as log-transformed fluorescence relative to normal preperfusion biopsies. Histology and CADI score were reported by a central pathology core lab at Massachusetts General Hospital (5, 6). Genes that correlated positively with CADI-12 and negatively with eGFR-12 were identified and ranked. Microarray data were deposited in GEO (accession no. GSE57387). eGFR was calculated using the modified diet in renal disease equation (MDRD) (47).

SHROOM3 SNP analysis. Targeted SNP genotyping for rs17319721 was done using Taqman SNP analysis assay (catalog no. 4351379, Applied Biosystems). DNA was extracted from preimplantation biopsies or blood for donor SNP and from peripheral blood for recipient SNP assay (20 ng/sample).

Cell culture. Human PRCECs (PromoCell), HK2 cells, and HEK-293T cells were cultured in Renal epithelial cell medium-2 (with supplement; catalog no. C-26130, Promocell), RPMI-1640, and DMEM (GIBCO), respectively. PRCECs at passage 5 or less were used for all studies. SHROOM3 transcript production in response to human TGF-β1 (R&D Biosystems) treatment was assayed by RT-PCR at 2.5, 5, or 10 ng/ml final concentration and AG-L-67051 treatment at 700 μM (catalog no. sc-222416, Santa Cruz Biotech) in nutrient-starved medium.

EMSA. HEK-293T cell nuclear extracts were prepared as described previously (48). EMSA probes were prepared by annealing complementary single-stranded oligonucleotides with 5′-GG overhangs (Sigma-Aldrich) and were labeled by filling in with [α-32P] dCTP using the Ready-To-Go kit (GE Healthcare, Amersham). Labeled probes (total length 36 bp each; Supplemental Table 6) were purified with G50 microcolumn (GE Healthcare, Amersham) following the manufacturer's protocol. EMSAs were performed as described previously, using 4 μg nuclear extracts/reaction. DNA binding complexes were separated by electrophoresis on a 4% polyacrylamide-Tris/glycine-EDTA gel for TCF7L2-supershift assays. Gels were dried and then exposed to X-ray film.

Promoter-enhancer reporter studies. A 24-bp sequence containing the putative TCF/LEF binding site from the first intron of *SHROOM3* (enhancer) was fused to a 3-kb promoter fragment encompassing 3,000 bp upstream of *SHROOM3*'s translational start site by PCR cloning. 2 variants of the promoter-enhancer sequence containing either the A or the G allele of rs17319721 were generated using 2 different forward PCR primers (Supplemental Table 6). Restriction sites for KpnI were introduced in forward primers, and for HindIII in the reverse primer. The PCR products were then cloned into luciferase reporter vector pGL3 Basic (catalog no. E-1751, Promega) using KpnI and HindIII sites. This generated 2 reporter constructs corresponding to the A or G allele enhancer sequence. Transient transfection of the A and G allele reporter constructs (1 μg each) with renilla luciferase reporter plasmid pTL-TK (200 ng) was carried out in HEK-293T cells plated on 6-well plates at 80% confluence using Polyjet reagent. After 24 hours, cells were lysed and protein extracted. Renilla and luciferase activity was measured in lysates using dual luciferase assay system (PJK Germany) on a microplate reader according to the manufacturer's protocol. Results were expressed as the luciferase/renilla ratio.

RT. Extracted biopsy RNAs were reverse transcribed using Sensiscript single-step RT (Qiagen) and Oligo-DT primer (Qiagen) with starting total RNA amount of 55 ng. Extraction samples with RNA concentrations <5 ng/μl by nanodrop were not used. For in vitro studies, we used Superscript-III (Invitrogen) with 500–1,000 ng starting total RNA.

RT-PCR. Intron-spanning primer sets were designed for *SHROOM3* using Primer-BLAST (NCBI), and PCR amplicons were confirmed by both melting curve analysis and agarose gel electrophoresis. *SHROOM3* expression was assayed in an internal and external cohort of patients by RT-PCR (Applied Biosystems 7500). Amplification curves were analyzed using the automated 7500 software platform via the ΔΔCt method. Human *GAPDH* was used as endogenous control. Similarly, primers were designed for human *COL1A1*. See Supplemental Table 8 for primer sequences.

WB. Cells were lysed with a buffer containing 1% Triton, a protease inhibitor mixture and tyrosine and serine/threonine phosphorylation and phosphatase inhibitors. Lysates were subjected to immunoblot analysis using polyclonal rabbit anti-SHROOM3 (gift from J. Hildebrand, University of Pittsburgh, Pittsburgh, Pennsylvania, USA), anti-V5 tag antibody (catalog no. R960-25, Invitrogen), phospho-SMAD3 antibody (rabbit polyclonal pS423/425), anti-SMAD3 (rabbit monoclonal SMAD3; catalog no. 9523, Epitomics), and anti-TCF7L2 (catalog nos. LC40C3 and 92G2, Cell Signalling). Densitometry was performed on WB images using ImageJ.

Overexpression studies. A human *SHROOM3* construct (Open Biosystems) was cloned into mammalian expression vector PC-DEST40 (Invitrogen) with C-terminal V5 and Histidine tags using the Clonase-II recombinase (Invitrogen) system. WT-TCF7L2 was cloned by PCR with LA polymerase (Clontech Laboratories Inc.), using oligo dT-primed cDNA from the HEK-293T human cell line as a template, and then subcloned into the pcDNA3.1$^+$ vector (Invitrogen). DN-TCF7L2, lacking the N-terminal 31 aa, was generated by PCR with WT-TCF7L2 plasmid described above as a template and then subcloned into the pcDNA3.1$^+$ vector (Invitrogen). Both WT-TCF7L2 and DN-TCF7L2 sequences were verified by DNA sequencing. Electroporative transfection using Lonza Nucleofector Technology (Basic Nucleofector kit for Primary Mammalian Epithelial Cells, Program T20) was used to transfect PRCECs and HK2 cells, as described previously (49). Forced

expression was confirmed by RT-PCR and WB with vector transfection as control. Profibrotic extracellular matrix markers were analyzed by RT-PCR. Effect of TGF-β1 treatment on matrix marker production in SHROOM3-transfected cells was assayed in nutrient-starved medium 36 hours after transfection. Phosphorylation of SMAD3 was measured at 5, 15, and 30 minutes of treatment with TGF-β1.

IF. PC-*SHROOM3* and PC-DEST40 transfected cells were plated in 12-cm wells on collagenized cover slips (20% rat-tail collagen; BD Biosciences) for 36–48 hours, formalin-fixed (36% HCHO and 0.1% Triton X100 in PBS). F-actin staining for cytoskeletal changes in SHROOM3-transfected cells was done using Cy5-conjugated phalloidin (Alexa Fluor 647 Phalloidin; Invitrogen) at 1:40 dilution in 1% BSA-PBS.

shRNA suppression studies. Human *SHROOM3* and *TCF7L2* short hairpin clones (Open Biosystems) were tested for optimal suppression by RT-PCR and WB in HEK-293T cells. The selected GFP-tagged hairpins were transfected into HEK-293T cells along with envelope plasmids using Polyjet (SignaGen labs) to generate a mammalian VSV-pseudotyped lentiviral expression construct. Cells were infected using these lentiviral constructs. Production of profibrotic matrix markers in response to TGF-β1 was measured in nutrient-starved medium at 24 hours. Phosphorylation of SMAD3 was assayed at 5, 15, and 30 minutes of TGF-β1 treatment after infection.

Tissue immunohistochemistry/IF. Slides were deparaffinized, treated with citrate buffer (pH 6), and blocked with goat serum/avidin for 20 minutes as previously described (49). Polyclonal rabbit anti-SHROOM3 antibody (1:100) incubation was done overnight at 4°C, followed by biotinylated goat anti-rabbit IgG and streptavidin-HRP treatments. For IF, snap-frozen kidney sections were formalin fixed and treated with anti-COL1A1 antibody (1:100 dilution; catalog no. 1310-01, Southern Biotech USA) overnight, and subjected to fluorescence microscopy.

Murine Shroom3 knockdown model. An shRNA guide sequence targeting *Shroom3* was selected based on in vitro *Shroom3* knockdown experiments in mouse kidney cell lines. A tetracycline-responsive, shRNAmir-mediated *Shroom3* knockdown mouse strain in a hybrid background (C57B6/129B) based on this shRNA guide sequence was developed in collaboration with Mirimus Inc. In the double-transgenic Rosa-RTTA mice, shRNAmir-mediated *Shroom3* knockdown was driven by the universal promoter ROSAm26 and inducible by Dox feeding. In the PAX8-RTTA animals, the shRNA expression was pantubular. Male mice were fed Dox for 3 weeks, then subjected to UUO to stimulate kidney fibrosis. Non-Dox-fed littermates with UUO were used as controls. At 10 days after UUO, kidney tissues were collected for histology, immunostaining for fibrosis markers, RNA isolation for RT-PCR, protein extraction for WB, and immunohistochemistry. 10 randomly selected high-power fields (hpfs; original magnification, ×40) were thresholded, and area of picrosirius red staining (paraffin-embedded sections) or COL1A1 staining (snap-frozen sections) was quantified and expressed as a percentage of total area using Metamorph (Molecular Devices) (49).

Statistics. Descriptive statistics (SEM and SD) were used to summarize the baseline characteristics of donors and recipients and were compared using χ^2 and Fisher's exact test. Univariate comparisons of continuous variables were done using unpaired *t* test (Mann-Whitney test for corresponding nonparametric analysis). Pearson's correlation was used to determine relationship between *SHROOM3* expression and eGFR and CADI score.

To determine the predictive factors of CADI-12≥2 outcome, multiple logistic regression using backward predictor selection was performed. The predictors assessed were as follows: donor age, donor race, donor gender, donor status, acute rejection before 3 months, recipient race, recipient gender, ECD, induction therapy, maintenance therapy, and presence of anti-HLA antibodies. CIT time and delayed graft function were also considered in a subgroup analysis that included deceased donors only. Logistic models using the same predictors were also built to assess predictive factors of progression by month 12 in the full transplant population and the deceased donor only population. Using multiple linear regression, the effects of these predictors on eGFR-12 were also assessed. All analyses were completed using SAS version 9.2 (SAS).

For in vitro experiments, unpaired *t* test was used to analyze data between 2 groups, and ANOVA followed by Bonferroni correction was used to compare more than 2 groups. Experiments were repeated at least 3 times to obtain SDs, and representative experiments are shown. Statistical significance was considered with 2-tailed *P* values less than 0.05.

Study approval. IRB approval for the human subjects in the study protocol was obtained from all 5 participating institutions, and informed written consent was obtained from all recipients and living donors. All animal studies were performed in accordance with guidelines and protocols approved by the IACUC at Icahn School of Medicine at Mount Sinai.

Acknowledgments

We thank Jeffrey Hildebrand for the rabbit anti-SHROOM3 antibody, the Shared Microscopy resource facility at Icahn School of Medicine at Mount Sinai, and Peter Heeger (Icahn School of Medicine at Mount Sinai) for critical reading and feedback. This work was supported by NIH grant 1U01AI070107 (to B. Murphy), an ASN Research Fellowship (to M.C. Menon), NIH grant 1R01DK098126 (to P.Y. Chuang), and NIH grants 1R01DK078897 and 1R01DK088541 (to J.C. He).

Address correspondence to: Barbara Murphy, Department of Medicine Icahn School of Medicine at Mount Sinai, One Gustave L Levy Place, New York, New York 10029, USA. Phone: 212.241.5850; E-mail: Barbara.murphy@mssm.edu.

1. Coresh J, et al. Prevalence of chronic kidney disease in the United States. *JAMA*. 2007;298(17):2038–2047.
2. Weiner DE, et al. Chronic kidney disease as a risk factor for cardiovascular disease and all-cause mortality: a pooled analysis of community-based studies. *J Am Soc Nephrol*. 2004;15(5):1307–1315.
3. Chapman JR, O'Connell PJ, Nankivell BJ. Chronic renal allograft dysfunction. *J Am Soc Nephrol*. 2005;16(10):3015–3026.
4. Nankivell BJ, Borrows RJ, Fung CL, O'Connell PJ, Allen RD, Chapman JR. The natural history of chronic allograft nephropathy. *N Engl J Med*. 2003;349(24):2326–2333.
5. Isoniemi HM, Krogerus L, von Willebrand E, Taskinen E, Ahonen J, Hayry P. Histopathological findings in well-functioning, long-term renal allografts. *Kidney Int*. 1992;41(1):155–160.
6. Yilmaz S, et al. Clinical predictors of renal allograft histopathology: a comparative study of single-lesion histology versus a composite, quantitative scoring system. *Transplantation*. 2007;83(6):671–676.
7. Magee JC, et al. Repeat organ transplantation in the United States, 1996–2005. *Am J Transplant*. 2007;7(5 pt 2):1424–1433.
8. Kottgen A, et al. Multiple loci associated with indices of renal function and chronic kidney disease. *Nat Genet*. 2009;41(6):712–717.
9. Boger CA, et al. Association of eGFR-related

Loci identified by GWAS with incident CKD and ESRD. *PLoS Genet*. 2011;7(9):e1002292.
10. Deshmukh HA, Palmer CN, Morris AD, Colhoun HM. Investigation of known estimated glomerular filtration rate loci in patients with Type 2 diabetes. *Diabet Med*. 2013;30(10):1230–1235.
11. Hildebrand JD, Soriano P. Shroom, a PDZ domain-containing actin-binding protein, is required for neural tube morphogenesis in mice. *Cell*. 1999;99(5):485–497.
12. Hildebrand JD. Shroom regulates epithelial cell shape via the apical positioning of an actomyosin network. *J Cell Sci*. 2005;118(pt 22):5191–5203.
13. Wortman B, Darbinian N, Sawaya BE, Khalili K, Amini S. Evidence for regulation of long terminal repeat transcription by Wnt transcription factor TCF-4 in human astrocytic cells. *J Virol*. 2002;76(21):11159–11165.
14. Henderson LJ, Narasipura SD, Adarichev V, Kashanchi F, Al-Harthi L. Identification of novel T cell factor 4 (TCF-4) binding sites on the HIV long terminal repeat which associate with TCF-4, β-catenin, and SMAR1 to repress HIV transcription. *J Virol*. 2012;86(17):9495–9503.
15. Brennan EP, et al. Next-generation sequencing identifies TGF-β1-associated gene expression profiles in renal epithelial cells reiterated in human diabetic nephropathy. *Biochim Biophys Acta*. 2012;1822(4):589–599.
16. Lan HY, Chung AC. TGF-β/Smad signaling in kidney disease. *Semin Nephrol*. 2012;32(3):236–243.
17. Gewin L, Zent R. How does TGF-β mediate tubulointerstitial fibrosis? *Semin Nephrol*. 2012;32(3):228–235.
18. Nishimura T, Takeichi M. Shroom3-mediated recruitment of Rho kinases to the apical cell junctions regulates epithelial and neuroepithelial planar remodeling. *Development*. 2008;135(8):1493–1502.
19. Xu T, Wu M, Feng J, Lin X, Gu Z. RhoA/Rho kinase signaling regulates transforming growth factor-β1-induced chondrogenesis and actin organization of synovium-derived mesenchymal stem cells through interaction with the Smad pathway. *Int J Mol Med*. 2012;30(5):1119–1125.
20. Premsrirut PK, et al. A rapid and scalable system for studying gene function in mice using conditional RNA interference. *Cell*. 2011;145(1):145–158.
21. Racusen LC, Regele H. The pathology of chronic allograft dysfunction. *Kidney Int Suppl*. 2010;(119):S27–S32.
22. Meier-Kriesche HU, Schold JD, Kaplan B. Long-term renal allograft survival: have we made significant progress or is it time to rethink our analytic and therapeutic strategies? *Am J Transplant*. 2004;4(8):1289–1295.
23. Lamb KE, Lodhi S, Meier-Kriesche HU. Long-term renal allograft survival in the United States: a critical reappraisal. *Am J Transplant*. 2011;11(3):450–462.
24. Flechner SM, et al. Kidney transplant rejection and tissue injury by gene profiling of biopsies and peripheral blood lymphocytes. *Am J Transplant*. 2004;4(9):1475–1489.
25. Hotchkiss H, et al. Differential expression of profibrotic and growth factors in chronic allograft nephropathy. *Transplantation*. 2006;81(3):342–349.
26. Mas V, et al. Establishing the molecular pathways involved in chronic allograft nephropathy for testing new noninvasive diagnostic markers. *Transplantation*. 2007;83(4):448–457.
27. Ju W, et al. Renal gene and protein expression signatures for prediction of kidney disease progression. *Am J Pathol*. 2009;174(6):2073–2085.
28. He W, Dai C, Li Y, Zeng G, Monga SP, Liu Y. Wnt/beta-catenin signaling promotes renal interstitial fibrosis. *J Am Soc Nephrol*. 2009;20(4):765–776.
29. Masszi A, et al. Integrity of cell-cell contacts is a critical regulator of TGF-β1-induced epithelial-to-myofibroblast transition: role for β-catenin. *Am J Pathol*. 2004;165(6):1955–1967.
30. Zheng G, et al. Disruption of E-cadherin by matrix metalloproteinase directly mediates epithelial-mesenchymal transition downstream of transforming growth factor-β1 in renal tubular epithelial cells. *Am J Pathol*. 2009;175(2):580–591.
31. Hindorff LA, et al. Potential etiologic and functional implications of genome-wide association loci for human diseases and traits. *Proc Natl Acad Sci U S A*. 2009;106(23):9362–9367.
32. ENCODE Project Consortium. An integrated encyclopedia of DNA elements in the human genome. *Nature*. 2012;489(7414):57–74.
33. Neph S, et al. An expansive human regulatory lexicon encoded in transcription factor footprints. *Nature*. 2012;489(7414):83–90.
34. Gerstein MB, et al. Architecture of the human regulatory network derived from ENCODE data. *Nature*. 2012;489(7414):91–100.
35. Nicolae DL, Gamazon E, Zhang W, Duan S, Dolan ME, Cox NJ. Trait-associated SNPs are more likely to be eQTLs: annotation to enhance discovery from GWAS. *PLoS Genet*. 2010;6(4):e1000888.
36. Andersson R, et al. An atlas of active enhancers across human cell types and tissues. *Nature*. 2014;507(7493):455–461.
37. The FANTOM Consortium and the RIKEN PMI and CLST (DGT). A promoter-level mammalian expression atlas. *Nature*. 2014;507(7493):462–470.
38. Thurman RE, et al. The accessible chromatin landscape of the human genome. *Nature*. 2012;489(7414):75–82.
39. Wang Q, et al. Cooperative interaction of CTGF and TGF-β in animal models of fibrotic disease. *Fibrogenesis Tissue Repair*. 2011;4(1):4.
40. Abreu JG, Ketpura NI, Reversade B, De Robertis EM. Connective-tissue growth factor (CTGF) modulates cell signalling by BMP and TGF-β. *Nat Cell Biol*. 2002;4(8):599–604.
41. Donauer J, et al. Expression profiling on chronically rejected transplant kidneys. *Transplantation*. 2003;76(3):539–547.
42. Ying L, Sarwal M. In praise of arrays. *Pediatr Nephrol*. 2009;24(9):1643–1659.
43. Akalin E, O'Connell PJ. Genomics of chronic allograft injury. *Kidney Int Suppl*. 2010;(119):S33–S37.
44. Ellis JW, et al. Validated SNPs for eGFR and their associations with albuminuria. *Hum Mol Genet*. 2012;21(14):3293–3298.
45. Sarwal M, et al. Molecular heterogeneity in acute renal allograft rejection identified by DNA microarray profiling. *N Engl J Med*. 2003;349(2):125–138.
46. Reeve J, et al. Diagnosing rejection in renal transplants: a comparison of molecular- and histopathology-based approaches. *Am J Transplant*. 2009;9(8):1802–1810.
47. Levey AS, Bosch JP, Lewis JB, Greene T, Rogers N, Roth D. A more accurate method to estimate glomerular filtration rate from serum creatinine: a new prediction equation. Modification of Diet in Renal Disease Study Group. *Ann Intern Med*. 1999;130(6):461–470.
48. Liu W, et al. AP-1 activated by toll-like receptors regulates expression of IL-23 p19. *J Biol Chem*. 2009;284(36):24006–24016.
49. Jin Y, et al. A systems approach identifies HIPK2 as a key regulator of kidney fibrosis. *Nat Med*. 2012;18(4):580–588.